Limnol. Oceanogr., 52(2), 2007, 820–832

Patterns in the $\delta^{13}C$ and $\delta^{15}N$ signature of *Ulva pertusa:* Interaction between physical gradients and nutrient source pools

Christopher D. Cornelisen,[1,2] *Stephen R. Wing, Kim L. Clark,*[1] *and M. Hamish Bowman*
Department of Marine Science, University of Otago, P.O. Box 56, Dunedin, New Zealand

Russell D. Frew
Department of Chemistry, University of Otago, P.O. Box 56, Dunedin, New Zealand

Catriona L. Hurd
Department of Botany, University of Otago, P.O. Box 56, Dunedin, New Zealand

Abstract

Field surveys and laboratory experiments were used to investigate the influence of the physical environment on variability in $\delta^{13}C$ and $\delta^{15}N$ signatures of *Ulva pertusa*, an abundant macroalgae inhabiting the low salinity layer (LSL) of Doubtful Sound, a New Zealand fjord. Field surveys revealed significant spatial variability in $\delta^{13}C$ (−18‰ to −12‰) and $\delta^{15}N$ (0‰ to 6‰). $\delta^{13}C$ was enriched at high irradiance sites and depleted at the fjord's wave-exposed entrance. $\delta^{15}N$ signatures increased from 0‰ at the fjord head where freshwater influence is greatest to an oceanic signature of 6‰ at the fjord entrance. $\delta^{15}N$ also increased by up to 4‰ between 2-m depth and the LSL–seawater interface (4-m depth); this pattern was less pronounced near the ocean. During laboratory experiments, $\delta^{13}C$ of *U. pertusa* became significantly enriched under high levels of irradiance (>50 μmol quanta m^{-2} s^{-1}). When exposed to high irradiance, increases in water motion rapidly depleted $\delta^{13}C$ signatures by as much as 5‰. Variability in $\delta^{13}C$ of *U. pertusa* in Doubtful Sound is largely a function of the light regime, which influences rates of photosynthesis and in turn the algae's dependence on HCO_3^-, an enriched source of carbon. However, increased water motion at the fjord entrance counteracts the influence of irradiance, leading to enhanced flux of CO_2 and depleted $\delta^{13}C$ signatures. Variation in $\delta^{15}N$ of *U. pertusa* is less dependent on the physical environment and instead is driven by the source pool signature, which in turn varies between freshwater and marine sources of nitrogen.

Our current understanding of food web dynamics has greatly benefited from the use of natural abundance isotope ratios of carbon ($^{13}C:^{12}C$) and nitrogen ($^{15}N:^{14}N$). Carbon isotope ratios (expressed as $\delta^{13}C$ in ‰) of consumers closely reflect those of their diet within 0‰ to 1‰ (DeNiro and Epstein 1978; McCutchan et al. 2003; Vanderklift and Ponsard 2003). Nitrogen isotope ratios ($\delta^{15}N$) exhibit a greater consumer enrichment that generally varies between 1.5‰ and 3.5‰ with each rise in trophic level (e.g., Vander Zanden and Rasmussen 2001; McCutchan et al. 2003; Vanderklift and Ponsard 2003). Many factors confound the ability to make accurate connections between consumers and their diet, including differences in consumer physiology and tissues and the presence of mixed diets that cover a range of $\delta^{13}C$ and $\delta^{15}N$ signatures (Vanderklift and Ponsard 2003). Studies aimed at understanding fractionation in consumer tissues (Hobson and Clark 1992; Vanderklift and Ponsard 2003) and incorporating variability in signatures associated with fractionation into mixing and mass balance models (Phillips and Koch 2002) address these issues; however, an overlooked source of uncertainty in food web studies is variability in isotope signatures among and within primary producers. Variability at the base of the food web is significant; a recent survey of macroalgae revealed a range of $\delta^{13}C$ values between −3 and −35 (Raven et al. 2002). Carbon signatures of an individual algae species (e.g., *Desmarestia antarctica*) can shift up to 20‰ with changes in the light regime (Wiencke and Fischer 1990).

Physiological studies along with field-based surveys in both marine (Raven et al. 1995; France and Holmquist 1997) and freshwater (Finlay et al. 1999) systems indicate that changes in the physical environment can induce significant isotopic variability in algae over relatively small spatial scales (on the order of meters). This potentially confounds the ability to link primary sources of carbon and consumers in a physically dynamic system. A mechanistic understanding of how signatures of primary producers vary spatially in response to changes in the physical environment

[1] Present address: Cawthron Institute, 98 Halifax Street East, Private Bag 2, Nelson, New Zealand.
[2] Corresponding author (chris.cornelisen@cawthron.org.nz).

Acknowledgments

We thank the numerous individuals who have contributed to the field component of this research, including E. Emmanuelli, R. McLeod, K. Rodgers, S. Rutger, E. Zydervelt, and especially P. Meredith. Technical support and assistance provided by staff at the Portobello Marine Laboratory, including D. Wilson, B. Dickson, and K. Boney, was greatly appreciated. We would also like to acknowledge R. Van Hale, K. Neal, and staff with Isotrace NZ limited for isotope analysis; S. Heesch for molecular analysis; and K. Currie for assistance with alkalinity measurements. Two anonymous reviews and input by J. Middelburg greatly improved the manuscript. This research was funded by an award from the Royal Society of New Zealand Marsden Fund to S.R.W. (U00213).

is required to enhance the resolution of ecosystem-wide studies, apply stable isotope analysis to fine-scale studies on diet and habitat use, and quantify the contributions of different primary producers to productivity at higher trophic levels (France and Holmquist 1997; Finlay et al. 1999).

Carbon and nitrogen isotope signatures of estuarine macroalgae depend largely on fractionation that occurs during physiological processes (nutrient assimilation) and the $\delta^{13}C$ and $\delta^{15}N$ signatures of dissolved nutrients. The surrounding physical environment, including gradients in irradiance, salinity, and water motion, will therefore have a large influence on the isotopic signatures of macroalgae. An increase in irradiance leads to a greater carbon demand and provides the needed energy for assimilating HCO_3^-, which is a more isotopically enriched source of carbon than CO_2 (aq). Thus, carbon isotope signatures for macroalgae capable of assimilating bicarbonate (HCO_3^-) can become elevated under increased levels of irradiance (Wefer and Killingley 1986; Kubler and Raven 1995). It is also possible that $\delta^{13}C$ and $\delta^{15}N$ signatures of estuarine macroalgae will vary along a salinity gradient. For instance, changes in salinity can affect carbon assimilation and carbonic anhydrase activity in macroalgae (Booth and Beardall 1991), which in turn may promote isotope fractionation. Changes in the forms of nutrients available to the algae and the isotope signatures of these nutrients also coincide with changes in salinity. For instance, the proportion of HCO_3^- to CO_2 (aq) increases with increasing salinity. In the case of nitrogen, both terrestrial and oceanic inputs of NH_4^+ and NO_3^- contribute to dissolved inorganic nitrogen (DIN) pools in estuarine waters. Signatures of nitrogen sources derived from rainwater, decomposition of terrestrial matter, or through nitrogen fixation are expected to be low ($\delta^{15}N \sim 0‰$; Natelhoffer and Fry 1988), whereas $\delta^{15}N$ of oceanic DIN containing remineralized NH_4^+ or upwelled NO_3^- are elevated in comparison ($\delta^{15}N \sim 8‰$; Wada et al. 1975; Sigman et al. 2000). Nitrogen isotope signatures of estuarine macroalgae will therefore be influenced by the availability of these different DIN sources, which in turn will vary along a gradient of salinity as a function of mixing between freshwater and marine source pools.

Field studies have demonstrated that water motion can also influence both carbon (France and Holmquist 1997; Finlay et al. 1999) and nitrogen (Trudeau and Rasmussen 2003) isotope signatures; however, its relative effect may vary depending on the physiological status of the algae (MacLeod and Barton 1998) or shifts in the amount or source of available nutrients (France and Holmquist 1997). Many estuarine macroalgae use both HCO_3^- and CO_2 (Raven et al. 1995), and the proportion of each of these sources assimilated at the thallus surface may depend on hydrodynamic regime (Beer and Eshel 1983; Hurd 2000).

The present study aims to quantify relationships between variation in isotope signatures ($\delta^{13}C$ and $\delta^{15}N$) of a common macroalgae species and physical attributes of its surrounding environment. The study focuses on *Ulva pertusa* in Doubtful Sound, New Zealand (Fig. 1), one of fourteen fjords within the region that exhibits sharp gradients in solar irradiance, salinity, and wave exposure.

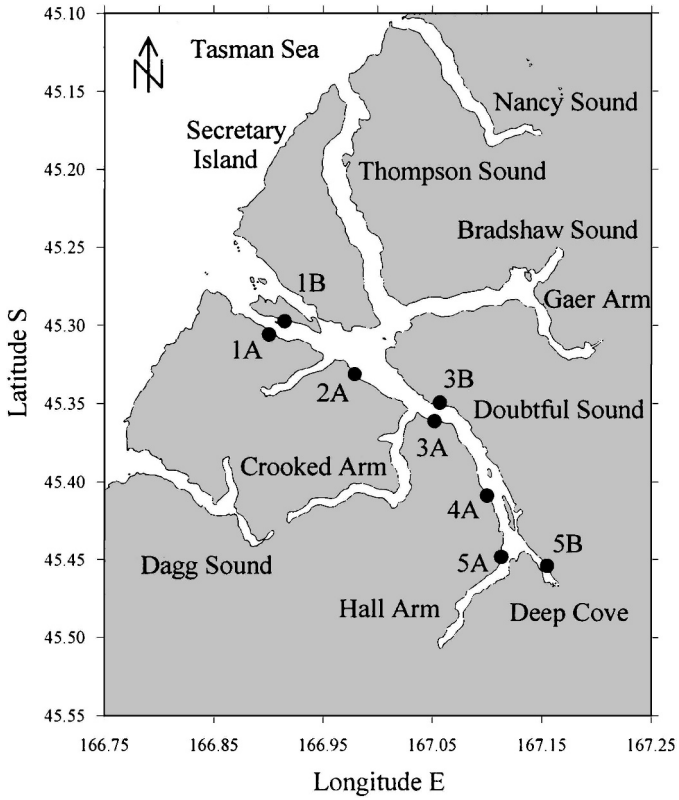

Fig. 1. Area map showing Doubtful Sound and collection sites along the north (A sites) and south (B sites) facing shores of the fjord.

In order to isolate the effects of irradiance on $\delta^{13}C$ and $\delta^{15}N$ under natural conditions, a series of field surveys are conducted at paired collection sites that receive low and high solar irradiance but are exposed to similar levels of salinity. In addition, sites are spaced evenly along the fjord axis between the fjord head and entrance to the ocean, which represents a strong gradient in salinity (a correlate to freshwater influence) and wave exposure. Laboratory experiments are conducted in order to isolate the effects of irradiance, salinity, and water motion on $\delta^{13}C$ and $\delta^{15}N$ signatures. These data are then used as a basis for understanding the variability in isotopic signatures observed in *U. pertusa* growing under different environmental conditions within Doubtful Sound.

Methods

Site selection—Eight field sites for data collection were selected that best represented the full range of solar irradiance, salinity, and wave exposure in Doubtful Sound (Fig. 1). A solar light model (r.sun) within version 5.0.3 of the Geographic Resources Analysis Support System (GRASS; http://grass.itc.it) was used for selecting sites at the lowest and highest range of irradiance at intervals along the fjord axis. The model provided estimates of integrated daily total solar irradiation (both direct and diffuse) taking into account the calculated solar transit and shadowing effects of fjord topography (Hofierka and Suri 2002). Model runs were summarized to create a map of total

annual solar irradiation providing an estimate of the relative incident surface irradiance at each site. Sites chosen based on these data included five north-facing sites that were spaced approximately 5–8 km apart between the head and entrance of the fjord (sites 1A, 2A, 3A, 4A, and 5A). Three additional sites (1B, 3B, and 5B) were located at a similar distance from the head of the fjord as their paired equivalents; however, they were positioned on the south-facing shore, which receives significantly less sunlight than the north-facing sites.

Site characterization—Irradiance was measured in situ using Odyssey light sensors (Dataflow Systems) deployed simultaneously at all sites between 23 March 2004 and 30 July 2004 and at the paired sites between 30 July 2004 and 20 January 2005. Sensors for measuring surface irradiance were placed 2 m above the high tide line to prevent fouling of the light sensor and in turn maximize the length of time they could be deployed. In order to obtain subsurface irradiance estimates and establish a relationship between surface irradiance and irradiance at the depth of algae collection, sensors were also deployed at 3-m depth at the six paired sites on 30 July 2004 and 29 September 2004. For sensors deployed underwater, data collected beyond the first 2 weeks of deployment were not used to prevent error associated with fouling of the light sensors. Each sensor was programmed to record integrated irradiance data over 10-min scan periods and was calibrated prior to deployment using a Licor light sensor.

Estimates of surface salinity at each of the sites were based on interpolation of the top 2 m of conductivity–temperature–depth (CTD) data collected along the axis of Doubtful Sound in 1998, 1999, 2002, and 2003. Salinity was interpolated between cast locations using a cost-based inverse true-distance interpolation, which allows the influence of physical barriers on water movement to be respected as well as the ability to constrain the area of confidence in a consistent manner. Salinity varies on much smaller time scales because of tides, mixing, and variability in freshwater inputs; however, the estimates provided typical differences in salinity among sites. Equivalent freshwater depth (EFD), an indication of the relative amount of freshwater in the water column at each site, was also estimated using the interpolated CTD data (Bowman 1978; Gibbs et al. 2000) and the following calculation:

$$\mathrm{EFD} = -z_0 + \int_0^{-Z_0} \frac{\rho(z)S(z)}{\rho_0 S_0} dz$$

where z_0 is the depth of the underlying reference layer of seawater, with salinity S_0 of 35 and density ρ_0 of 1,025 kg m^{-3}.

Predicted local variability in average wave height among collection sites was used as a proxy for water motion. Wave climate was described using the simulating waves nearshore (SWAN) wave model (Booij et al. 1999). Boundary conditions for the model were provided from a 20 yr hindcast of regional wind and wave parameters produced by a regional wave model (Gorman et al. 2003). Wave climatology was estimated at 50-m resolution and forced by regional wind predictions from the European Centre for Medium Range Weather Forecasts.

In order to assess the influence of source pool signature on $\delta^{13}C$ variation in *U. pertusa,* the $\delta^{13}C$ of the total dissolved inorganic carbon (DIC) pool was determined for water samples collected on 24 September 2006 at three locations along the fjord (1A, 3A, and 5B). At each site, three replicate water samples were collected at depths of 1, 3, and 5 m, and one sample was collected at 10-m depth. A Van Dorn style water sampler (3 liters) was used to collect each sample, from which two subsamples were retained; a 100-mL sample for determination of $\delta^{13}C$ of the DIC and a 1-liter sample for determination of alkalinity. CTD casts were collected simultaneously with water samples in order to measure temperature and salinity at the depths of sample collection. Total alkalinity in micromoles per kilogram was determined using an automated, closed-cell, potentiometric titration procedure (Dickson and Goyet 1994). Carbon isotope signatures of DIC in water samples were measured by extraction of DIC as gaseous carbon dioxide using phosphoric acid, followed by analysis of the CO_2 by isotope ratio mass spectrometry (IRMS).

Field collections—Samples of *U. pertusa* were collected during 5 months in 2004: 26–30 January, 22–26 March, 24–28 May, 26–30 July, and 27–30 September. Samples collected at the sampling sites were identified as the same species based on morphological characteristics as well as DNA sequencing (Heesch and Broom unpubl. data). At each site, five individual thalli were collected haphazardly between 2- and 4-m depth, which represents the depth band in which *U. pertusa* is commonly found in Doubtful Sound (Clark unpubl. data). It is noted that *U. pertusa* grows slightly deeper at site 3A and that samples at this sight were collected between 2 and 5 m. In order to evaluate variability in isotope signatures that occurs with depth, *U. pertusa* was also collected at 2-, 3-, and 4-m depth at all sites (except site 1B) during March and at paired sites during September. Depths were relative to the high tide line (tidal range 1.5 m) and were determined using a depth gauge. Samples were kept in water from their site of collection during transport back to the field station, where tissue samples were then placed in 1.7-mL microtubes and frozen. Samples were stored at $-80^{\circ}C$ until they were processed for isotopic analysis.

Laboratory experiments—In order to investigate the combined effects of irradiance and salinity on isotope fractionation, a controlled experiment was completed at the University of Otago's Portobello Marine Laboratory in April 2004. *U. pertusa* collected in Doubtful Sound were placed in three salinity treatments (5, 14, and 35), which were in turn placed within one of two irradiance treatments (full and shaded sunlight). In order to evaluate potential effects of site history on fractionation, *U. pertusa* used in the experiment included thalli from two different sites; 1A, a site with high irradiance and salinity typical of seawater, and 5B, a site with low irradiance and low salinity (*see Fig. 1*). Whole thalli from the two sites were collected on 26 March 2004 and transported to the Portobello Marine

Laboratory (8 h away) in aerated buckets of seawater. The algae were placed in a shaded outdoor holding tank for 4 d with flowing seawater until the experiment began on 01 April 2004.

Thirty thalli from each of the two sites were trimmed to approximately 6 g wet weight and cleaned of epiphytes. Pairs of thalli (consisting of one from each site) were then placed in 5-liter clear plastic bins. A section of plastic mesh fencing (1 cm^2 pore size) fixed in the center of each bin was used to separate paired samples. Five replicate bins were used for each salinity and irradiance treatment (30 bins total). The three salinity treatments were prepared by mixing filtered seawater with purified freshwater. Seawater was pumped from Otago Harbor and filtered with ultraviolet light to minimize presence of microorganisms within the bins that could potentially affect nutrient concentrations. Bins were aerated continuously and water changes were carried out every 3 to 4 d. A modified version of F2 media (Guillard and Ryther 1962) was used as a nutrient source; sodium nitrate was replaced with ammonium sulfate and reduced to half the concentration ($\sim$90 μmol L^{-1}) to avoid any toxic effects of high ammonium levels. Salinity was monitored between water changes, and if necessary freshwater added to minimize salinity fluctuations due to evaporation. All 30 bins were randomly placed in a large hydroponics tray with flow-through seawater that provided temperature control ($\pm 1^{\circ}C$) among bins. Fifteen of the bins (five from each salinity treatment) were kept under three layers of 50% shade cloth that reduced irradiance to approximately 10% ambient levels; the bins received full sun throughout the day. Over the course of the experiment, average daily irradiance measured with Odyssey light sensors was 12.6×10^6 μmol quanta m^{-2} d^{-1} (peak surface irradiance = 170 to 1,300 μmol quanta m^{-2} s^{-1}) for the irradiance treatment and 1.2×10^6 μmol quanta m^{-2} d^{-1} (peak surface irradiance = 15 to 150 μmol quanta m^{-2} s^{-1}) for the shaded treatment. Bins were routinely rotated to vary their position within the experimental setup.

Once every 5 to 7 d, wet weights for each thalli were measured for calculating specific growth rates using the equation specific growth (% growth d^{-1}) = 100 ln $(W_t/W_0)/t$, where W_0 = initial wet weight, W_t = final wet weight, and t = time (days) (D'Elia and Deboer 1978). Water on the surface of the algae was removed via centrifugation (20 spins in a salad spinner) prior to weighing. Each thalli was trimmed after weighing to maintain relatively constant biomass in all the bins. Samples of tissue ($\sim$1 g wet weight) for isotope analysis were collected along the distal edge of six random plants at the beginning of the experiment and from each of the experimental plants after 30 d. Tissues were stored frozen ($-80^{\circ}C$) until sample processing.

A series of four flume experiments were completed between 01 March and 17 April 2005 to assess the effect of water motion and the interactive effects of water motion and irradiance on $\delta^{13}C$ and $\delta^{15}N$ signatures. Three identical flumes, each 600 liters in volume, were used to expose *U. pertusa* to a range of flow conditions. Water flow in each flume was generated by a 1 hp motor and drive shaft with propeller. The main working sections of the flumes were constructed of clear Plexiglas measuring 2.4-m long by 0.4-m wide and 0.4-m deep. Each flume was filled to a depth of 0.3 m and received continuous flowing seawater ($\sim$10 liters min^{-1}) from Otago Harbor. For three experiments, each flume was set at a different mainstream velocity, with one running at a low velocity ($\bar{U}$ = 0.8 cm s^{-1}), one at a moderate velocity ($\bar{U}$ = 5.1 cm s^{-1}), and one at a high velocity ($\bar{U}$ = 25.4 cm s^{-1}). An acoustic Doppler velocimeter (Sontek 10 MHz field ADV) was used to measure mainstream velocity. The velocity used in each flume was alternated for each experiment. Irradiance was provided by full spectrum 36 W Phillips Aqua Relle tubes set on a 12 h on/off cycle. Water temperature was routinely recorded and concentrations of water-column nutrients (NH_4^+, NO_3^-, and PO_4^{3+}) were measured on three occasions to ensure variables other than water flow were constant between treatments.

During the course of each experiment, 8 to 12 thalli from site 3A were equally spaced midwater in each flume by affixing individual thalli to rigid plastic rods that hung vertically into the water column. In order to investigate interactive effects between irradiance and water motion on isotope signatures, half of the thalli in each flume were exposed to a high level of irradiance (55 μmol quanta m^{-2} s^{-1} measured at the depth of the thalli) while the other half were exposed to reduced irradiance (10 μmol quanta m^{-2} s^{-1}). Irradiance was reduced by laying shade cloth over half of each flume's working area. In order to obtain additional information along a velocity gradient, a fourth experiment was run using two of the flumes, with one set at a mean velocity of 2.5 and one at a mean velocity of 12.4 cm s^{-1}. Irradiance levels for this experiment were set at 55 μmol quanta m^{-2} s^{-1}. Each of the above experiments lasted 10 d, after which tissue samples from each thalli were collected, weighed, and immediately processed for isotope analysis. Specific growth rates were determined using the same methods as those used in the irradiance and salinity experiment.

Sample processing—Tissue samples from both field collections and laboratory experiments were dried for 48 h at $60^{\circ}C$, homogenized into a fine powder using a mortar and pestal, and stored in a desiccator until isotopic analysis. All samples were analyzed using an elemental analyzer (Carlo Erba NC 2500) coupled to an isotope ratio mass spectrometer (Europa Hydra) to determine percentage N and percentage C in the tissue and $^{15}N:^{14}N$ and $^{13}C:^{12}C$ ratios. Data were converted to δ notation based on the ratio of heavy to light isotope in the sample (R_s) relative to the standard atmospheric air for nitrogen and Vienna PeeDee Belemnite (VPDB) for carbon (R_{std}): δ (‰) = $(R_s - R_{std})/R_{std} \times 1{,}000$. Precision was 0.2‰ for $\delta^{13}C$ and 0.3‰ for $\delta^{15}N$ based on one standard deviation of replicate samples.

Data analysis—Analysis of variance was used to assess spatial differences in isotope signatures among the eight sites. Two-way ANOVA was used to evaluate differences in signatures according to site locations along the fjord axis and between those positioned on north versus south-facing

walls of the fjord. For the outdoor experiment, two-way ANOVA was used to test the factors irradiance and salinity and their interaction on $\delta^{13}C$ and $\delta^{15}N$. Regression analysis and ANOVA were used to the test the effects of water motion and interactive effects of water motion and irradiance on isotope signatures, respectively.

Results

Site characterization—Monthly averages of daily surface irradiance ranged between a low of 1.3×10^6 μmol quanta m^{-2} d^{-1} in June and high of 6.6×10^6 μmol quanta m^{-2} d^{-1} in December along the south-facing shore and between a low of 3.3×10^6 μmol quanta m^{-2} d^{-1} and high of 23.3×10^6 μmol quanta m^{-2} d^{-1} along the north-facing shore during these same months (Fig. 2A). Average daily surface irradiance over the course of a year at sites situated on the south-facing shore was significantly lower than irradiance received at north-facing sites (Fig. 2B). Data collected 3 m below the surface of the water reflected measures of surface irradiance. Regressions of surface to subsurface irradiances at each of the paired sites were significant ($p < 0.001$, r^2 0.80 to 0.95) and indicated that surface irradiance was attenuated by 80% (range 79–82%) at 3 m below the surface. Based on the estimated attenuation, typical maxima for irradiances at 3-m depth and during winter months (June–September) ranged between 50 and 300 μmol m^{-2} s^{-1} along the north-facing shore and between 5 and 30 μmol m^{-2} s^{-1} along the south-facing shore. In summer months (December–March) at this same depth, maxima ranged between 100 and 500 μmol m^{-2} s^{-1} and between 10 and 50 μmol m^{-2} s^{-1} for the north- and south-facing shores, respectively.

Surface salinity estimated from a series of CTD surveys ranged from 8 near the fjord head to 22 near the fjord entrance (Fig. 2C). EFD ranged between a high of 2.3 m and a low of 1.1 m along the salinity gradient (Fig. 2D); thus freshwater influence within the region of the rock wall colonized by *U. pertusa* is greatest toward the head of the fjord and decreases with proximity to the ocean entrance. Estimates of significant mean wave height (H_{sig}) indicated that the two sites near the entrance to the ocean (sites 1A and 1B) are influenced by oceanic waves. Modeled estimates of H_{sig} at sites 1A and 1B were 0.15 m and 0.14 m, respectively. Estimates of H_{sig} for the remaining sites were negligible (<0.1 m).

Total alkalinity for water samples collected over a depth gradient and at three sites along the axis of the fjord ranged between a low of 657 (±16) μmol kg^{-1} in the surface water in Deep Cove (site 5B) and a high of 2,248 μmol kg^{-1} at 10-m depth near the ocean entrance (Site 1A) (Fig. 3A). For all sites, alkalinity was lowest in the surface water and increased to values typical of seawater below the low salinity layer (LSL) (10-m depth). Therefore, *U. pertusa* at 2-m depth is exposed to lower concentrations of HCO_3^- than algae at 4-m depth. The difference in alkalinity, and therefore HCO_3^- concentration, between 2- and 4-m depth is pronounced at the head of the fjord where freshwater influence is the greatest (Fig. 3A).

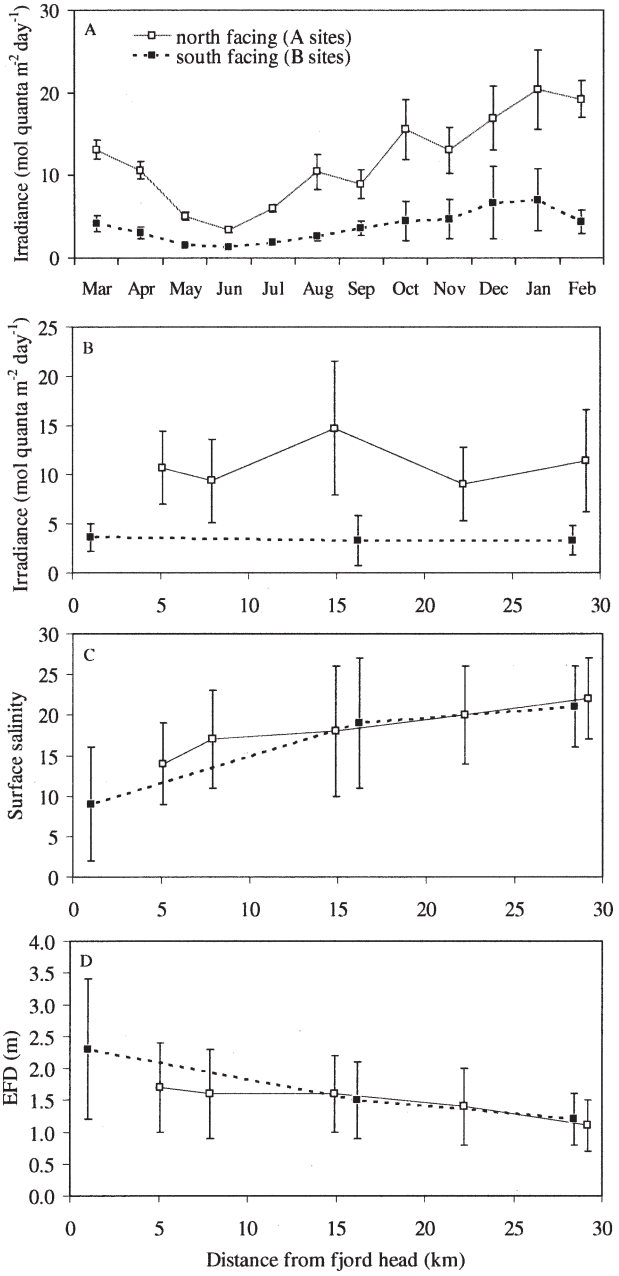

Fig. 2. (A) Average daily surface irradiance between March 2004 and March 2005 for five sites situated along the north-facing shore and three sites along the south-facing shore. (B) Average daily surface irradiance for each site over the course of a year. (C) Salinity in the surface water (top 1 m) based on the average of three CTD casts. (D) EFD based on salinity data collected from three CTD casts. Error bars ±1 SD. Sites are shown with reference to their distance from the fjord head (Deep Cove).

Carbon signatures for DIC in water samples showed a similar pattern to alkalinity over a depth gradient at the three sites (Fig. 3B). DIC $\delta^{13}C$ ranged between a low of −3.3‰ (±0.4) at 1-m depth at the head of the fjord (Site 5B) and high of 0.2‰ at 10-m depth at the fjord entrance (site 1A). The similar spatial pattern in DIC $\delta^{13}C$ to that of alkalinity demonstrates how a higher contribution of HCO_3^- to the DIC pool results in a higher $\delta^{13}C$ DIC

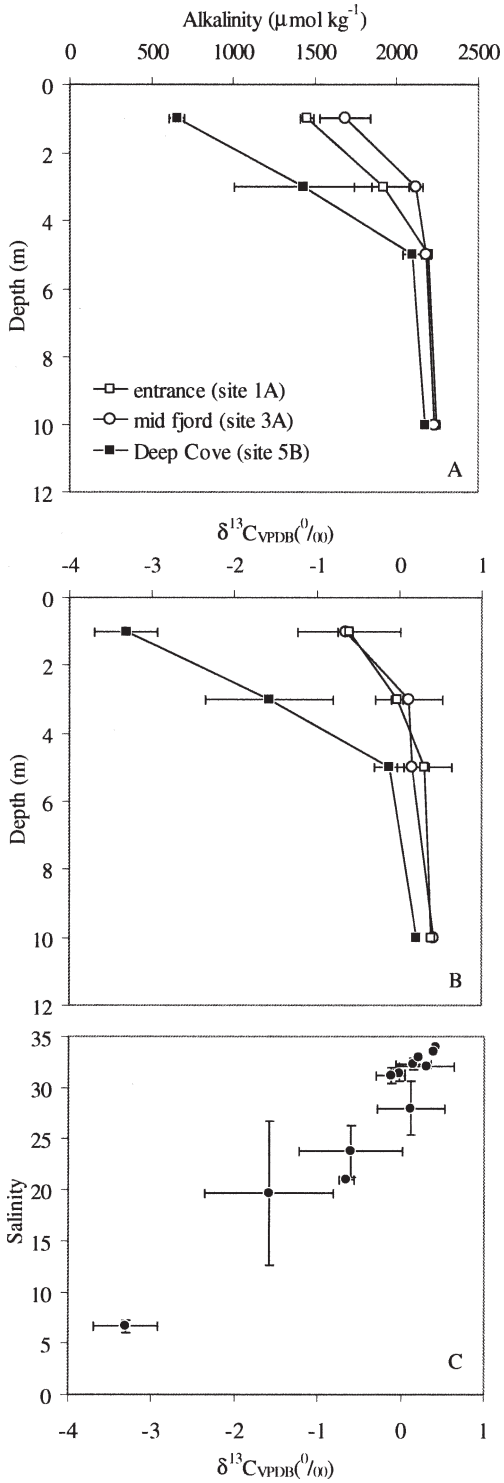

Fig. 3. (A) Depth profiles of total alkalinity, (B) $\delta^{13}C$ of the total dissolved inorganic carbon (DIC), and (C) the relationship between salinity (based on CTD casts) and DIC $\delta^{13}C$. Data are means (±1 SD) of replicate water samples ($n = 3$) and CTD casts ($n = 3$) collected at three locations (Sites 1A, 3A, and 5B) along the axis of the fjord.

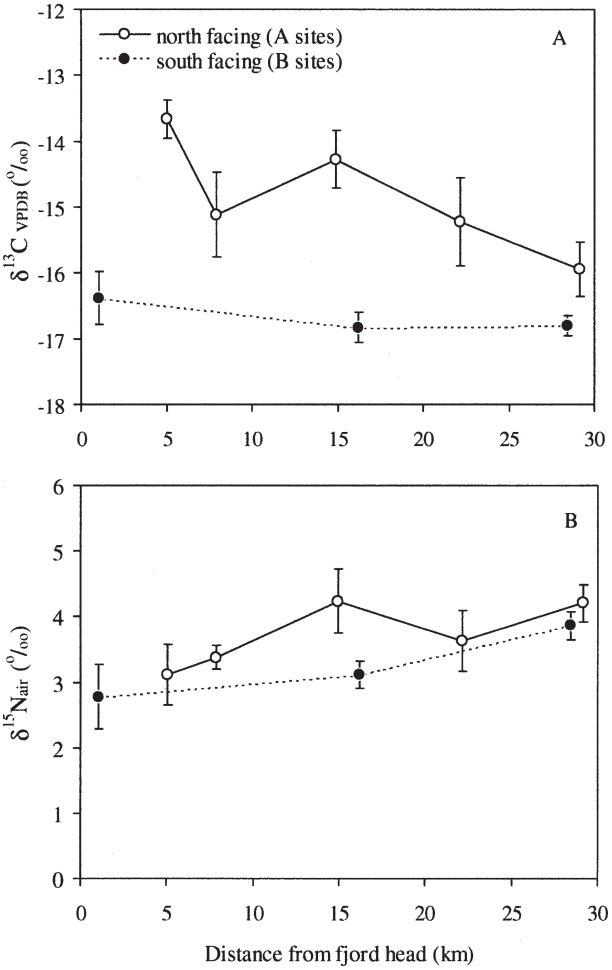

Fig. 4. (A) $\delta^{13}C$ and (B) $\delta^{15}N$ signatures for *Ulva pertusa* collected along the north-facing shore (A sites) and south-facing shore (B sites). Data represent the average of monthly means for each site (±1 SE, $n = 5$ for paired sites and $n = 4$ for sites 2 and 4).

value. Conversely, the relative contribution of CO_2 (aq) to the total DIC pool is highest in the surface water and near the fjord head, where $\delta^{13}C$ DIC is lowest. Based on water temperatures, the predicted fractionation for ^{13}C between bicarbonate and CO_2 was estimated to range between 9.1‰ at 7.0°C (surface water at site 5B) and 9.8‰ at 12.5°C (temperature of underlying seawater; Zhang et al. 1995). The relationship between salinity and DIC $\delta^{13}C$ demonstrates how the relative abundance of HCO_3^- and CO_2 varies along a salinity gradient, both with depth and along the fjord axis.

Spatial variation in isotope signatures—Carbon signatures for *U. pertusa* collected in Doubtful Sound ranged between −18.2‰ (site 3B in July) and −12.0‰ (site 5A in January). $\delta^{13}C$ signatures followed a general pattern of higher $\delta^{13}C$ signatures along the north-facing shore and lower signatures along the south-facing shore (Fig. 4A). During all five sampling months, $\delta^{13}C$ values were significantly higher for algae collected at sites along the north-facing shore than for those collected along the south-facing shore (Table 1). The difference in $\delta^{13}C$ between

Table 1. Results from two-factor ANOVA used to test north vs. south facing location, position along the axis of the fjord, and the interaction between the two factors on carbon and nitrogen signatures of *Ulva pertusa*. Two samples were collected for site 1B in January and March; therefore, results for these months are based on paired sites at locations 3 and 5. All other results are based on replicate samples ($n = 5$) collected at the three paired sites (1A–1B, 3A–3B, and 5A–5B) during each month.

			Month of collection				
Signature	Factor		Jan 2004	Mar 2004	May 2004	Jul 2004	Sep 2004
$\delta^{13}C$	North vs. south facing	MS	14.48	17.38	38.24	36.73	101.89
		F	18.56	42.71	208.93	194.89	117.00
		p	<0.001	<0.001	<0.001	<0.001	<0.001
	Along-axis position	MS	1.16	5.78	6.19	2.36	14.07
		F	1.49	14.14	33.79	12.54	16.16
		p	0.240	0.001	<0.001	<0.001	<0.001
	Interaction	MS	0.59	4.10	11.27	2.06	2.61
		F	0.76	10.08	61.60	10.94	15.32
		p	0.398	0.005	<0.001	<0.001	<0.001
$\delta^{15}N$	North vs. south facing	MS	1.19	15.15	3.14	2.61	1.90
		F	0. 81	16.37	11.90	15.32	7.85
		p	0.381	<0.001	0.003	<0.001	0.007
	Along-axis position	MS	8.79	5.09	0.75	0.23	2.77
		F	5.98	5.50	2.84	1.36	11.45
		p	0.026	0.029	0.085	0.275	<0.001
	Interaction	MS	5.19	1.97	2.69	0.34	11.50
		F	3.53	2.12	10.20	1.97	47.50
		p	0.079	0.160	0.001	0.162	<0.001

shores tended to decrease with increasing proximity to the ocean entrance (Fig. 4A). Results from a two-factor ANOVA using pooled data for paired sites were consistent with those run with data from individual months (Table 1) and showed a significant effect of along-axis position (df = 2, MS = 4.61, $F = 6.19$, $p = 0.007$), cross-fjord position (df = 1, MS = 31.3, $F = 42.12$, $p \ll 0.001$), and interaction between the two factors (df = 2, MS = 2.65, $F = 3.56$, $p = 0.044$). Interaction is most evident at the fjord entrance, where wave action is greatest (site 1A).

Nitrogen signatures for *U. pertusa* ranged between 0.1‰ (site 4A in March) and 6‰ (site 1A in March). $\delta^{15}N$ signatures increased with increasing distance from the fjord head and were generally higher along the north-facing shore than along the south-facing shore (Fig. 4B). Variation in $\delta^{15}N$ between shores was greatest between midfjord sites. These differences were statistically significant for four of the five sampling months (Table 1). Based on pooled averages for all sampling months (Fig. 4B), there were significant effects of cross-fjord (df = 1, MS = 2.71, $F = 4.66$, $p = 0.041$) and along-axis (df = 2, MS = 3.09, $F = 5.32$, $p = 0.012$) position; however, there was no significant interaction between the two factors ($p = 0.43$).

Carbon signatures varied up to 1.5‰ between 2 and 4 m; however, there was no consistent pattern with depth over the length of the fjord (Figs. 5A and 6A). A decrease in the $\delta^{13}C$ signature of *U. pertusa* with depth contradicts the pattern in the DIC $\delta^{13}C$ signature, which increased with depth (Fig. 3B). $\delta^{15}N$ signatures demonstrated a clear pattern with depth; $\delta^{15}N$ was lightest in the surface water and increased by 3‰ between 2- and 4-m depth (Fig. 5A, 6B). The variability over the depth interval decreased with proximity to the ocean entrance (Fig. 5B). Differences in $\delta^{15}N$ between 2 and 4 m were most pronounced at the fjord head (Fig. 6B), which is also where the EFD is greatest (Fig. 2D).

Temporal variation in isotope signatures—Carbon signatures of *U. pertusa* showed significant differences according to sampling month (df = 4, MS = 2.89, $F = 2.94$, $p = 0.046$). $\delta^{13}C$ was least negative in January, a period of high irradiance, and most negative during July, a period of low irradiance (*see Fig. 2A*, *Fig. 7A*). There was no significant interaction between cross-fjord sampling location and the month of collection (df = 4, MS = 0.16, $F = 0.17$, $p = 0.95$), indicating that differences in $\delta^{13}C$ for *U. pertusa* collected along north versus south-facing shores were relatively consistent over time. There was also a significant difference in $\delta^{15}N$ signatures between sampling months (df = 4, MS = 2.16, $F = 3.69$, $p = 0.021$); however, they displayed no clear temporal pattern (Fig. 7B).

Irradiance and salinity experiment—Carbon signatures of *U. pertusa* from Doubtful Sound were strongly influenced by irradiance and less so by salinity, which coincides with the $\delta^{13}C$ signature of DIC available to the algae (Fig. 8A). There was no significant difference based on the site of origin of the *U. pertusa* used in the experiments (1A near the entrance of the fjord vs. 5B at the head of the fjord); therefore, isotope values for the two thalli in each bin were averaged for statistical analysis. Prior to the start of the experiment, carbon signatures were the same for *U. pertusa* from the two sites (mean = −13.7‰, SD = 0.5‰ for site 5B and 0.9‰ for site 1A). After 30 d, carbon signatures were significantly enriched by 4‰ for thalli exposed to full sun compared with thalli grown under reduced irradiance (Fig. 8A; df = 1, MS = 96.1, $F = 194.6$, $p < 0.001$). $\delta^{13}C$ was also significantly different among salinity treatments, with values decreasing

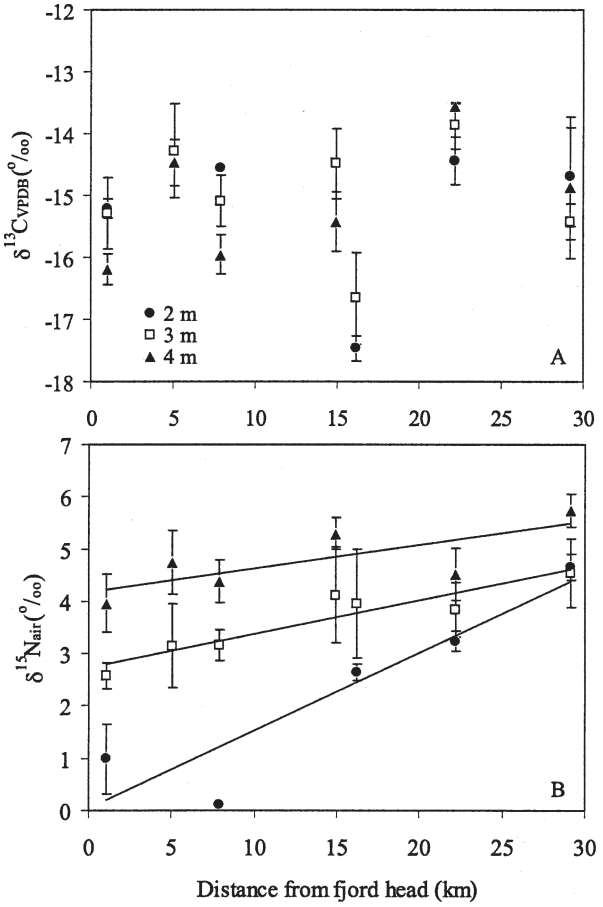

Fig. 5. Mean (A) $\delta^{13}C$ and (B) $\delta^{15}N$ signatures for *Ulva pertusa* samples collected in March 2004 according to depth of collection and distance from the fjord head. Error bars represent ±1 SD ($n = 4$). The point without error bars represents the mean of two samples. There was a significant relationship between $\delta^{15}N$ versus distance from the fjord head for *U. pertusa* collected at 2 m (slope = 0.15, intercept = 0.05, $r^2 = 0.85$, $p = 0.025$) and at 3 m (slope = 0.06, intercept = 2.74, $r^2 = 0.86$, $p = 0.003$).

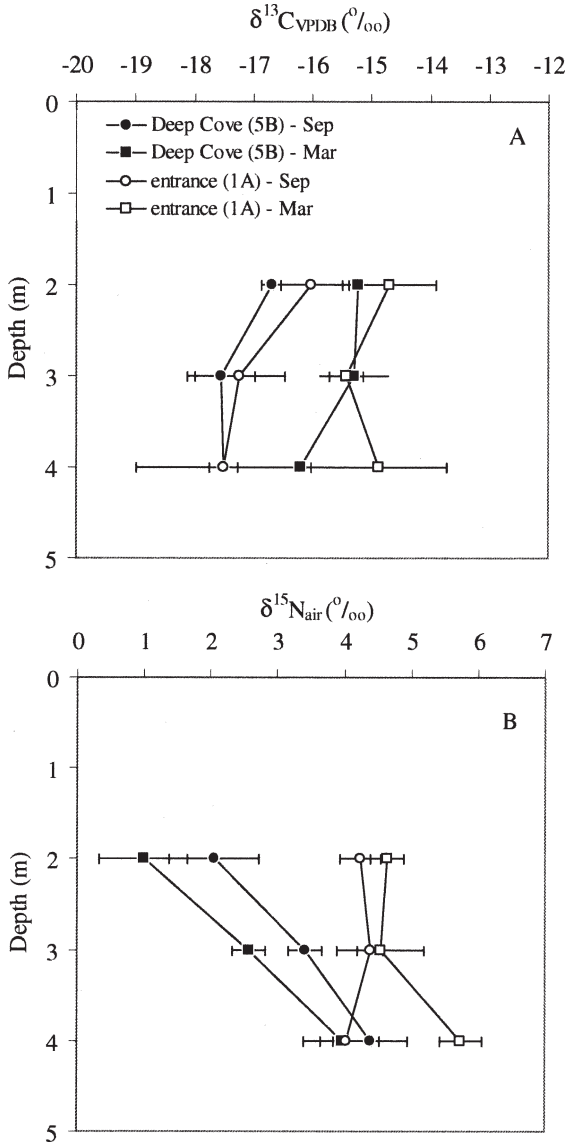

Fig. 6. Mean (A) $\delta^{13}C$ and (B) $\delta^{15}N$ signatures (±1 SD) over a depth gradient at the fjord head (site 5B) and at the entrance (site 1A) during late winter (September 2004) and late summer (March 2004).

by 1‰ to 2‰ from low to high salinity (df = 2, MS = 7.6, $F = 15.5$, $p < 0.001$). There was no significant interaction between irradiance and salinity on $\delta^{13}C$ ($p = 0.74$).

Both irradiance and salinity significantly influenced the nitrogen signature of *U. pertusa*. $\delta^{15}N$ signatures were consistently depleted by 1.7‰ to 2.6‰ in the high irradiance treatment across the range of salinity. In addition, $\delta^{15}N$ signatures decreased by 1.5‰ from low to high salinity. A mass balance of nitrogen during the experiment revealed that significant fractionation occurred as a function of growth rate and changes in NH_4^+ concentration, which in turn was a consequence of the closed experimental design. Growth rates for *U. pertusa* exposed to full sun (mean = 3.36% d^{-1}, SD 0.74) were over twice as high as those for *U. pertusa* exposed to reduced irradiance (mean = 1.32% d^{-1}, SD 0.76). Salinity had no effect on specific growth rates.

Flume experiments—Irradiance and water motion significantly influenced $\delta^{13}C$ signatures of *U. pertusa*. For thalli exposed to an irradiance of 55 μmol m^{-2} s^{-1}, there was a significant nonlinear decline in $\delta^{13}C$ signatures from a high of −13.1‰ (SD ± 0.43) at low velocity to a low of −18.0‰ (SD ± 0.51) at high velocity ($\delta^{13}C = -1.33 \ln U_b - 13.974$, $r^2 = 0.87$, $p = 0.02$, Fig. 8B). Under reduced irradiance, water velocity had no significant effect on $\delta^{13}C$ signatures. At low velocity, $\delta^{13}C$ signatures for *U. pertusa* were enriched by 3.5‰ for thalli grown under an irradiance 55 μmol m^{-2} s^{-1} than for those grown under 10 μmol m^{-2} s^{-1} (Fig. 8B). The difference in $\delta^{13}C$ between irradiance treatments declined with an increase in velocity and actually reversed at high velocity, which demonstrates interaction between the factors irradiance and water motion.

Nitrogen isotope signatures were significantly higher (by 0.2‰ to 0.9‰) for *U. pertusa* grown under the high

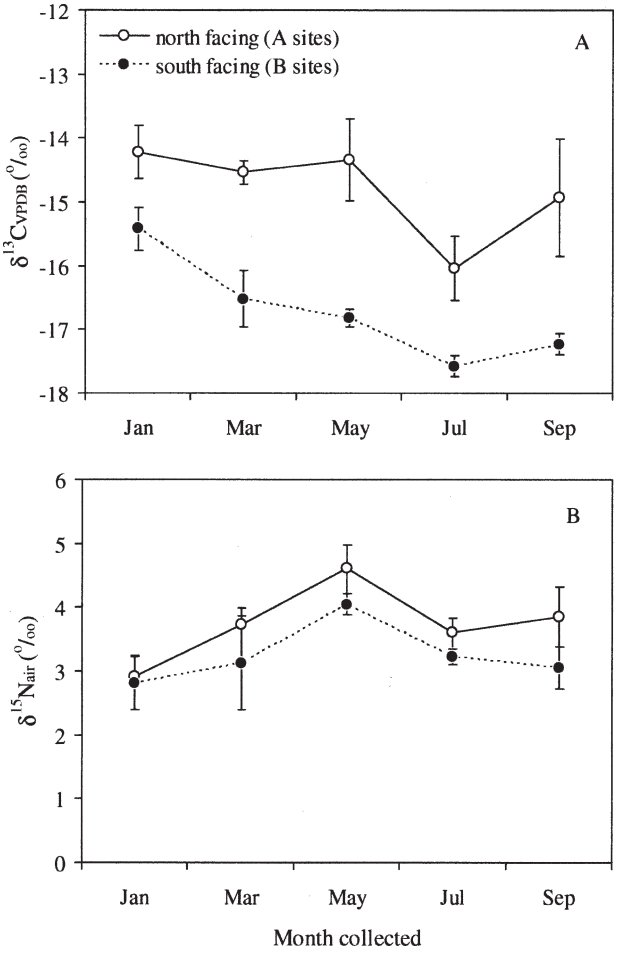

Fig. 7. Average (A) δ^{13}C and (B) δ^{15}N signatures for *Ulva pertusa* collected along the north-facing shore (A sites) and south-facing shore (B sites) according to sampling month. Data points represent the average among sites for each shore (±1 SE, $n = 5$ sites for the north-facing shore and three sites for the south-facing shore).

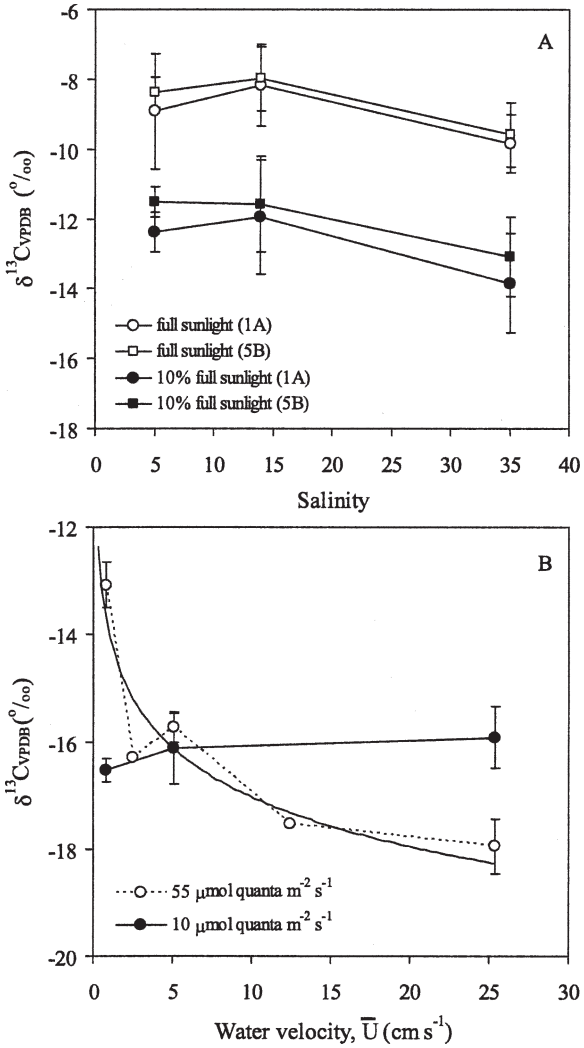

Fig. 8. (A) Mean δ^{13}C (±1 SD, $n = 5$) for *Ulva pertusa* grown for 30 d under three different salinity treatments and under full sunlight (avg. daily irradiance = 12.6×10^6 μmol quanta m^{-2} d^{-1}) or 10% full sunlight (avg. daily irradiance = 1.2×10^6 μmol quanta m^{-2} d^{-1}). Two thalli, one from site 5B and one from site 1A, were placed in each container. (B) δ^{13}C for *U. pertusa* grown for 10 d in three flumes under low (0.8 cm s^{-1}), moderate (5.1 cm s^{-1}), and high (25.4 cm s^{-1}) velocity and exposed to low (10 μmol m^{-2} s^{-1}) or high (55 μmol m^{-2} s^{-1}) irradiance. Data are the average (±1 SE) of means from four experiments (*see Methods*). Also shown are mean values for six thalli exposed to 2.5 cm s^{-1} and 12.4 cm s^{-1} at high irradiance. There was a significant nonlinear decline (solid line) in δ^{13}C with an increase in velocity under the high irradiance treatment ($\delta^{13}C = -1.38 \ln U - 13.81$, $r^2 = 0.87$, $p = 0.02$).

irradiance treatment than for those exposed to reduced irradiance (Fig. 9A). Water velocity had no significant effect on δ^{15}N signatures. The percentage of *Ulva* tissue composed of nitrogen was dependent on both irradiance and water velocity. At low velocity percentage N was 1% higher for thalli grown under low irradiance. Increased velocity enhanced percentage N within the tissue, particularly for thalli exposed to high irradiance where it doubled from a low of 2.2% N to a high of 4.1% N over the range of velocity (Fig. 9B). At high velocity, percentage N was similar between the two irradiance treatments. Specific growth rates during the flume experiments ranged between 1.1% and 3.1% d^{-1} under low irradiance and between 8.7% and 12.2% d^{-1} under high irradiance and were not dependent on water flow for either irradiance treatment.

Discussion

Variability in δ^{13}C signatures of *U. pertusa* is driven by the interactive effects of irradiance and water motion, which in turn influence the form of dissolved inorganic carbon assimilated by the algae. In contrast, δ^{15}N signatures of *U. pertusa* showed clear patterns along the fjord axis and over a depth gradient that were consistent with expected changes in the available source and signature of dissolved inorganic nitrogen assimilated by the algae. Laboratory experiments confirmed that increased irradiance leads to enriched carbon signatures in *U. pertusa* (as high as −8.0‰). These results are consistent with previous studies (Wiencke and Fischer 1990; Kubler and Raven 1995) and suggest that *U. pertusa* from

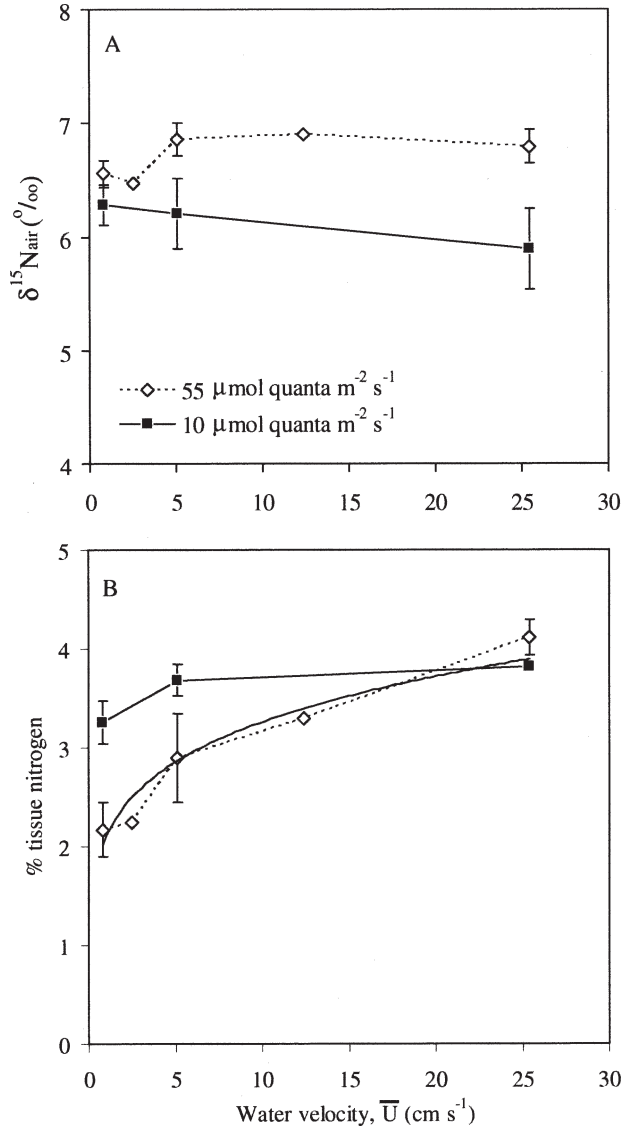

Fig. 9. (A) *Ulva pertusa* grown for 10 d in three flumes under low (0.8 cm s^{-1}), moderate (5.1 cm s^{-1}), and high (25.4 cm s^{-1}) velocity and exposed to low (10 μmol m^{-2} s^{-1}) or high (55 μmol m^{-2} s^{-1}) irradiance. Data are the average (±1 SE) of means from four experiments (*see Methods*). Also shown are mean values for six thalli exposed to 2.5 cm s^{-1} and 12.4 cm s^{-1} at high irradiance. (B) Percentage tissue N in *U. pertusa* over the range of velocity and two light treatments. The solid line shows the significant dependence of percentage tissue N on water velocity under the high irradiance treatment (%N = $2.10U^{0.19}$, $r^2 = 0.92$, $p = 0.008$).

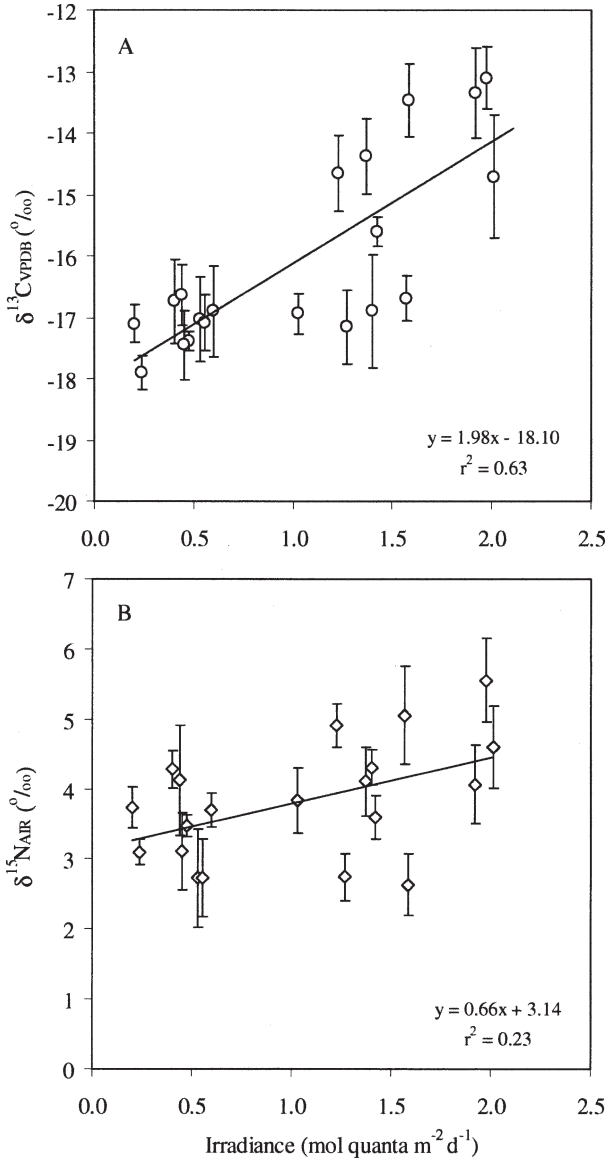

Fig. 10. Mean (A) $\delta^{13}C$ and (B) $\delta^{15}N$ signatures of *Ulva pertusa* as a function of irradiance at each of the sites in which samples were collected and irradiance data were available (±1 SD, $n = 5$). Average daily irradiance is based on continuous data collected at the surface for 14 d prior to sample collection, which was then corrected for 3-m depth using estimates of attenuation (irradiance at 3 m is approximately 20% of the surface irradiance).

Doubtful Sound is capable of efficient HCO_3^- use (Raven et al. 2002). Shifts in $\delta^{13}C$ associated with a changing light regime are most likely linked to changes in photosynthetic rates and the amounts of HCO_3^- versus CO_2 used to meet carbon demands (Raven et al. 1995).

The pattern of $\delta^{13}C$ signatures in the field suggest that *U. pertusa* thalli along the shaded south-facing shore meet lower carbon demands through diffusive entry of CO_2, while those along the north-facing shore often receive saturating levels of irradiance (Koch 1993) and depend on active uptake of HCO_3^-. An alternative explanation is that increased irradiance leads to higher efficiency in intracellular CO_2 fixation irrespective of the original carbon source, which in turn could elevate $\delta^{13}C$ signatures due to increased retention of ^{13}C within the cell. While this may partially explain the observed differences, it is not entirely consistent with results from the field or those obtained from the flume experiments that demonstrate interactions between the effects of irradiance and water motion.

Gradients in average irradiance explain approximately 63% of the variability in *Ulva* $\delta^{13}C$ signatures (Fig. 10A), which indicates that other factors are contributing to variability in $\delta^{13}C$. Despite exposure to similar levels of

irradiance, $\delta^{13}C$ for thalli collected at site 1A (located at the wave-exposed entrance) were consistently more negative (up to 3‰) than those for thalli collected at site 5A (located near the fjord head). Carbon signatures of *U. pertusa* did not reflect changes in the DIC $\delta^{13}C$ signature associated with a salinity gradient; therefore, depleted $\delta^{13}C$ signatures at the entrance are most likely due to increased water motion. Results from the flume experiments corroborated this conclusion and demonstrated that an increase in water velocity depresses the $\delta^{13}C$ signature of *U. pertusa* when levels of irradiance exceed 50 μmol quanta m^{-2} s^{-1}. In Doubtful Sound, this level of irradiance translates to $\sim 1 \times 10^6$ μmol quanta m^{-2} d^{-1}, above which considerable variability in $\delta^{13}C$ is observed (*see Fig. 10A*). If we remove points for site 1A from the figure, the relationship between irradiance and $\delta^{13}C$ is greatly improved ($r^2 = 0.85$).

An increase in water motion enhances flux of CO_2 to the thalli, which results in a greater contribution of CO_2 to total DIC uptake than if the algae were exposed to high levels of irradiance and low-flow conditions (Beer and Eshel 1983; France and Holmquist 1997). Thus, $\delta^{13}C$ is more negative in a high irradiance–high flow environment (e.g., site 1A) than a high irradiance–low-flow environment (e.g., site 5A). This explanation is consistent with the concept of mass-transfer limitation. The flux (m) of CO_2 can be described by the equation $m = \beta(C_b - C_w)$, where β is the mass-transfer coefficient and $(C_b - C_w)$ represents the gradient between the CO_2 concentration in the water column (C_b) and concentration at the thallus surface (C_w) (Bilger and Atkinson 1992; Dade 1993). Under saturating levels of irradiance, we can assume that the rate at which *U. pertusa* processes CO_2 will exceed the rate of CO_2 delivery to the algae ($C_b \gg C_w$). In other words, flux is limited by the rate of delivery (mass-transfer limited). This is a safe assumption because of the limited availability of CO_2 versus HCO_3^- in marine systems and because there are no energy requirements for CO_2 uptake. Under this scenario, flux of CO_2 into the thallus will be dependent on bulk concentration of CO_2 (assumed to be relatively constant) and β. The mass-transfer coefficient is in turn influenced by changes in the diffusivity (D) of CO_2 (minimal temperature effects) and the thickness of the diffusive boundary layer (l) ($\beta = D/l$). Based on typical water temperatures in Doubtful Sound, the $\delta^{13}C$ of CO_2 is expected to be 9‰ to 10‰ more depleted than the $\delta^{13}C$ of HCO_3^- (Mook et al. 1974; Zhang et al. 1995). Therefore, in order to obtain signatures that are 3‰ more depleted than expected, *U. pertusa* at site 1A need only meet 30% to 40% of its carbon requirements by passively assimilating CO_2. This explanation is plausible given previous information on the amount of required carbon that can be met with CO_2 (Beer and Eshel 1983).

Temporal variation in $\delta^{13}C$ with seasonal fluctuations in irradiance are also expected and to some degree observed in Doubtful Sound. Seasonal changes in water motion throughout the fjord may explain why temporal variation in $\delta^{13}C$ was not more pronounced (e.g., greater enrichment in $\delta^{13}C$ in January). Long-term wind data collected in Deep Cove indicate that average wind speeds are greatest during the summer months (e.g., average = 12 km h^{-1} in January vs. 2 km h^{-1} in July; University of Otago unpubl. data). If we assume wind-generated surface waves accompany this trend, then there may be a seasonal effect of water flow on $\delta^{13}C$ signatures. Spatial and temporal characterization of hydrodynamic regime, along with flume experiments conducted over a full range of velocity, is warranted to refine relationships between irradiance, water flow, and carbon isotope signatures.

In contrast to $\delta^{13}C$ signatures, the body of evidence suggests that $\delta^{15}N$ signatures of *U. pertusa* in Doubtful Sound reflect the source pool signature and are less dependent on irradiance and water motion. As a result, $\delta^{15}N$ will be more closely linked to processes influencing the source(s) of DIN available to the algae. A gradient in irradiance explained only 23% of the natural variability in $\delta^{15}N$ (*see Fig. 10B*), and there was no pattern in $\delta^{15}N$ signatures with seasonal changes in irradiance. However, unlike $\delta^{13}C$, there were clear patterns in $\delta^{15}N$ both along the fjord axis and with depth that coincided with the structure of the LSL and degree of mixing between freshwater inputs and the underlying seawater.

The LSL often extends below 4 m at the head of the fjord and becomes shallower and more mixed with the underlying seawater toward the fjord entrance (Gibbs et al. 2000). *U. pertusa* with the greatest exposure to freshwater inputs, including those located closest to the fjord head and at 2-m depth, exhibited signatures between 0‰ and 2‰, which is in the range of ammonium associated with rainwater and river outflow (Hoering 1957; Wada et al. 1975; Natelhoffer and Fry 1988). Signatures for *U. pertusa* collected at the fjord entrance and those at a depth of 4 m were between 4‰ and 6‰, which closely reflect the average signature of oceanic nitrate (4.5‰ to 5‰; Altabet et al. 1999). These data are consistent with a previous study that demonstrated elevated $\delta^{15}N$ in macroalgae exposed to pulses of oceanic nitrate (Leichter et al. 2003). Surveys of water-column nutrients have also demonstrated a greater contribution of ammonium to the total DIN pool in the surface waters and a greater presence of nitrate in the underlying seawater (Cornelisen unpubl. data; Goebel et al. 2005).

The differences in $\delta^{15}N$ observed during flume experiments likely resulted from differences in growth rates among irradiance treatments and the extent to which tissue nitrogen came into equilibrium with the signature of the DIN in seawater originating from Otago Harbor. *Ulva* species inhabiting Otago Harbor typically exhibit elevated $\delta^{15}N$ signatures (range 7‰ to 10‰) compared with *U. pertusa* collected in Doubtful Sound (Cornelisen unpubl. data). In the field, *U. pertusa* grows slightly deeper at site 3A (3 to 5 m) than the other sites (Clark 2005); closer proximity to the underlying seawater may explain why $\delta^{15}N$ for *U. pertusa* collected at this site was significantly higher than those for *U. pertusa* collected on the south-facing shore (*see Fig. 3B*). While our results are consistent with the idea that $\delta^{15}N$ is driven by the source pool signature, we must consider that many factors can influence the fractionation of $\delta^{15}N$ in both source pools and within the tissues of primary producers (Robinson 2001). Determination of $\delta^{15}N$ signatures of DIN would assist in identifying the extent to which additional factors may be influencing $\delta^{15}N$ signatures of *U. pertusa*.

Implications of findings for food web studies—The extent of variation in both $\delta^{13}C$ (−18‰ to −12‰) and $\delta^{15}N$ (0‰ to 6‰) observed for *U. pertusa* greatly exceeds predicted levels of isotope enrichment between a consumer and its diet (e.g., Vander Zanden and Rasmussen 2001). Isotope variability in *U. pertusa* therefore has important implications for food web studies conducted in Fiordland and other estuarine systems in which this widely distributed species is found. There are several primary sources of carbon that form the base of the food web in Fiordland, including terrestrial inputs via frequent landslides, phytoplankton blooms (Goebel et al. 2005), microphytobenthos, and over 100 species of macroalgae (Nelson et al. 2002). *U. pertusa* is the most abundant macroalgae species within the LSL of Doubtful Sound, comprising up to 40% of the total biomass of macroalgae within the top 4 m of the water column (Clark 2005). Large isotopic variability in a dominant primary producer such as *U. pertusa* could therefore limit the ability to link higher trophic levels and specific primary sources of carbon within a physically dynamic ecosystem, particularly if samples were collected over varying spatial and temporal scales.

Identifying patterns in isotope variability in dominant macroalgal species along environmental gradients will expand the application of stable isotopes to food web studies at finer spatial scales. Macroalgae along the fjord walls has been identified as a primary carbon source to grazers and higher trophic level organisms (Lamare and Wing 2001; Lusseau and Wing 2006). Identification of spatial patterns in isotope signatures of macroalgae will in turn provide information on habitat use and movement of these organisms across the landscape. For instance, we might expect macroalgal grazers that keep to the same area and suspension feeders attached to the fjord walls to reflect observed patterns in $\delta^{13}C$ and $\delta^{15}N$ in *U. pertusa*. Conversely, patterns would be less detectable in those species that use several habitats throughout the fjord. Our study emphasizes the close link between isotopic variability in primary producers and the surrounding physical environment. By understanding relationships between the two, we greatly increase our ability to determine the fate of terrestrial and marine sources of nutrients and quantify the contributions of different sources of primary carbon to aquatic food webs.

References

Altabet, M. A., C. Pilskaln, R. Thunell, C. Pride, D. Sigman, F. Chavez, and R. Francois. 1999. The nitrogen isotope biogeochemistry of sinking particles from the margin of the Eastern North Pacific. Deep-Sea Res. **46:** 655–679.

Beer, S., and A. Eshel. 1983. Photosynthesis of *Ulva* sp. II. Utilization of CO_2 and HCO^-_3 when submerged. J. Exp. Mar. Biol. Ecol. **70:** 99–106.

Bilger, R. W., and M. J. Atkinson. 1992. Anomalous mass transfer of phosphate on coral reef flats. Limnol. Oceanogr. **37:** 261–272.

Booij, N., R. C. Ris, and L. H. Holthuijsen. 1999. A third-generation wave model for coastal regions, Part I, model description and validation. J. Geophys. Res. Oceans **104:** 7649–7666.

Booth, W. A., and J. Beardall. 1991. Effects of salinity on inorganic carbon utilization and carbonic-anhydrase activity in the halotolerant alga *Dunaliella salina* (Chlorophyta). Phycologia **30:** 220–225.

Bowman, M. J. 1978. Spreading and mixing of the Hudson River effluent into the New York Bight, p. 373–386. *In* J. C. Nihoul [ed.], Hydrodynamics of estuaries and fjords. Elsevier.

Clark, K. 2005. Physical factors influencing macroalgal community structure and productivity in Doubtful Sound, Fiordland. M.S. thesis, Univ. of Otago.

Dade, W. B. 1993. Near-bed turbulence and hydrodynamic control of diffusional mass transfer at the sea floor. Limnol. Oceanogr. **38:** 52–69.

D'elia, C. F., and J. A. Deboer. 1978. Nutritional studies of two red algae. II. Kinetics of ammonium and nitrate uptake. J. Phycol. **14:** 266–272.

Deniro, M. J., and S. Epstein. 1978. Influence of diet on the distribution of carbon isotopes in animals. Geochim. Cosmochim. Acta **42:** 495–506.

Dickson, A. G., and C. Goyet. 1994. Handbook of methods for the analysis of the various parameters of the carbon dioxide system in sea water, Ver. 2. U.S. DOE ORNL/CDIAC-74. Oak Ridge National Laboratory, Tennessee.

Finlay, J. C., M. E. Power, and G. Cabana. 1999. Effects of water velocity on algal carbon isotope ratios. Limnol. Oceanogr. **44:** 1198–1203.

France, R. L., and J. G. Holmquist. 1997. $\delta^{13}C$ variability of macroalgae: Effects of water motion via baffling by seagrasses and mangroves. Mar. Ecol. Prog. Ser. **149:** 305–308.

Gibbs, M. T., M. J. Bowman, and D. E. Dietrich. 2000. Maintenance of near-surface stratification in Doubtful Sound, New Zealand Fjord. Estuar. Coast. Shelf Sci. **51:** 683–704.

Goebel, N. L., S. R. Wing, and P. W. Boyd. 2005. A mechanism for onset of diatom blooms in a fjord with persistent salinity stratification. Estuar. Coast. Shelf Sci. **64:** 546–560.

Gorman, R. M., K. R. Bryan, and A. K. Laing. 2003. A wave hind-cast for the New Zealand region—deep water wave climate. NZ J. Mar. Freshw. Res. **37:** 589–612.

Guillard, R. R., and J. H. Ryther. 1962. Studies on marine planktonic diatoms. I. *Cyclotella nana* Hustedt and *Detonala confervaceae* (Cleve) Gran. Can. J. Microbiol. **8:** 229–239.

Hobson, K. A., and R. W. Clark. 1992. Assessing avian diets using stable-carbon and nitrogen isotopes. II. Factors influencing diet-tissue fractionation. Condor **94:** 189–197.

Hoering, T. C. 1957. The isotopic composition of ammonia and the nitrate ion in rain. Geochim. Cosmochim. Acta **12:** 97–102.

Hofierka, J., and M. Suri. 2002. The solar radiation model for Open source GIS: Implementation and applications, p. 1–19. *In*: Proceedings of the Open source GIS/GRASS users conference, 11–13 September 2002. M. Ciolli and P. Zatelli [eds.] Univ. Trento. Trento, Italy.

Hurd, C. L. 2000. Water motion, marine macroalgal physiology, and production. J. Phycol. **36:** 453–472.

Koch, E. W. 1993. The effect of water flow on photosynthetic processes of the alga *Ulva lactuca* L. Hydrobiology **260/261:** 457–462.

Kubler, J. E., and J. A. Raven. 1995. The interaction between inorganic carbon acquisition and light supply in *Palmaria palmata* (Rhodophyta). J. Phycol. **31:** 369–375.

Lamare, M. D., and S. R. Wing. 2001. Calorific content of New Zealand marine macrophytes. NZ J. Mar. Fresh. Res. **35:** 335–341.

Leichter, J. J., H. L. Stewart, and S. L. Miller. 2003. Episodic nutrient transport to Florida coral reefs. Limnol. Oceanogr. **48:** 1394–1407.

Lusseau, S. M., and S. R. Wing. 2006. Importance of local production versus pelagic subsidies in the diet of an isolated population of bottlenose dolphins *Tursiops* sp. Mar. Ecol. Prog. Ser. **321:** 283–293.

MacLeod, N. A., and D. R. Barton. 1998. Effects of light intensity, water velocity, and species composition on carbon and nitrogen stable isotope ratios in periphyton. Can. J. Fish. Aquat. Sci. **55:** 1919–1925.

McCutchan, J. H., W. M. Lewis, C. Kendall, and C. C. McGrath. 2003. Variation in trophic shift for stable isotope ratios of carbon, nitrogen, and sulfur. Oikos **102:** 378–390.

Mook, W. G., J. C. Bommerso, and W. H. Staverma. 1974. Carbon isotope fractionation between dissolved bicarbonate and gaseous carbon-dioxide. Earth Planet. Sci. Lett. **22:** 169–176.

Natelhoffer, K. J., and B. Fry. 1988. Controls on natural Nitrogen-15 and Carbon-13 abundances in forest soil organic matter. J. Am. Soil Sci. Soc. **52:** 1633–1640.

Nelson, W. A., E. Villouta, K. F. Neill, G. C. Williams, N. M. Adams, and R. Slivsgaard. 2002. Marine macroalgae of Fiordland, New Zealand. Tuhinga **13:** 117–152.

Phillips, D. L., and P. L. Koch. 2002. Incorporating concentration dependence in stable isotope mixing models. Oecologia **130:** 114–115.

Raven, J. A., J. Beardall, A. M. Johnston, J. E. Kubler, and I. Geoghegan. 1995. Inorganic carbon acquisition by *Hormosira banksii* (phaeophyta, fucales) and its epiphyte *Notheia anomala* (phaeophyta, fucales). Phycologia **34:** 267–277.

———, and others. 2002. Mechanistic interpretation of carbon isotope discrimination by marine macroalgae and seagrasses. Funct. Plant Biol. **29:** 355–378.

Robinson, D. 2001. δ^{15}N as an integrator of the nitrogen cycle. Trends Ecol. Evol. **16:** 153–162.

Sigman, D. M., M. A. Altabet, D. C. McCorkle, R. Francois, and G. Fischer. 2000. The delta N-15 of nitrate in the Southern Ocean: Nitrogen cycling and circulation in the ocean interior. J. Geophys. Res. Oceans **105:** 19599–19614.

Trudeau, V., and J. B. Rasmussen. 2003. The effect of water velocity on stable carbon and nitrogen isotope signatures of periphyton. Limnol. Oceanogr. **48:** 2194–2199.

Vanderklift, M. A., and S. Ponsard. 2003. Sources of variation in consumer-diet δ^{15}N enrichment: A meta-analysis. Oecologia **136:** 169–182.

Vander Zanden, M. J., and J. B. Rasmussen. 2001. Variation in δ^{15}N and δ^{13}C trophic fractionation: Implications for aquatic food web studies. Limnol. Oceanogr. **46:** 2061–2066.

Wada, E., T. Kadonaga, and S. Matsuo. 1975. ^{15}N abundance in nitrogen of naturally occurring substances and global assessment of denitrification from isotopic viewpoint. Geochem. J. **9:** 139–148.

Wefer, W., and H. S. Killingley. 1986. Carbon isotopes in organic matter from a benthic alga *Halimeda incrassata* (Bermuda): Effects of light intensity. Chem. Geol. **59:** 321–326.

Wiencke, C., and G. Fischer. 1990. Growth and stable carbon isotope composition of cold-water macroalgae in relation to light and temperature. Mar. Ecol. Prog. Ser. **65:** 283–292.

Zhang, J., P. D. Quay, and D. O. Wilbur. 1995. Carbon isotope fractionation during gas-water exchange and dissolution of CO_2. Geochim. Cosmochim. Acta **59:** 107–114.

Received: 24 July 2006
Accepted: 24 October 2006
Amended: 24 November 2006